

Excitation Pathways in Resonant Inelastic X-Ray Scattering of Solids

Christian Vorwerk,^{1,2,*} Francesco Sottile,^{3,4} and Claudia Draxl^{1,4}

¹Physics Department and IRIS Adlershof, Humboldt-Universität zu Berlin, Berlin, Germany

²European Theoretical Spectroscopy Facility (ETSF)

³LSI, Ecole Polytechnique, CNRS, CEA, Institut Polytechnique de Paris, F-91128 Palaiseau, France

⁴European Theoretical Spectroscopic Facility (ETSF)

(Dated: March 2, 2020)

We present a novel derivation of resonant inelastic x-ray scattering (RIXS) which yields an expression for the RIXS cross section in terms of emission pathways between intermediate and final many-body states. Thereby electron-hole interactions are accounted for, as obtained from full diagonalization of the Bethe-Salpeter equation within an all-electron first-principles framework. We demonstrate our approach with the emission spectra of the fluorine K edge in LiF, and provide an in-depth analysis of the pathways that determine the spectral shape. Excitonic effects are shown to play a crucial role in both the valence and core regime.

Resonant inelastic x-ray scattering (RIXS) spectroscopy is an important tool to unravel the nature of elementary excitations. RIXS has been measured to study excitations in a wide range of crystalline materials [1–4] and molecules [5–7]. Theoretically, the microscopic RIXS process is commonly described in a two-step model [1, 2]: In the first step, an incoming x-ray photon with energy ω is absorbed, leading to the excitation of a tightly bound core electron to the conduction band. Subsequently, a valence electron fills the core hole by emitting an x-ray photon with smaller energy ω' . The system thus reaches a many-body state with a hole in a valence state and an excited electron in a conduction state. This final state is similar to a final state of optical absorption. The two processes within RIXS occur coherently, *i.e.* the entire process cannot simply be considered as an absorption followed by an emission [8, 9]. Rather, the final state of the absorption process determines the possible emission processes. Through this coherence, RIXS spectroscopy offers an element- and orbital-selective probe of elemental electronic excitations, because the absorption edge can be selected such to allow for emission from specific valence states only.

The rich information contained in RIXS spectra has stimulated *ab initio* descriptions of the microscopic processes. First-principles approaches for RIXS in solids have been derived with various levels of sophistication, starting with the independent-particle approximation (IPA) within density functional theory (DFT) [8, 10–13]. Treatment of the electron-hole interaction in the core-hole approximation led to an improvement [14] but still does not capture the full picture. Electron-hole correlation plays a crucial role in RIXS even in weakly correlated materials, as both the intermediate and the final excited state of the process contain an electron-hole pair. This situation demands a more accurate approach as provided within many-body perturbation theory by the solution of the Bethe-Salpeter equation (BSE)[15–19]. This method is the state-of-the-art for the calculation of optical and x-ray absorption spectroscopy of condensed matter [20–

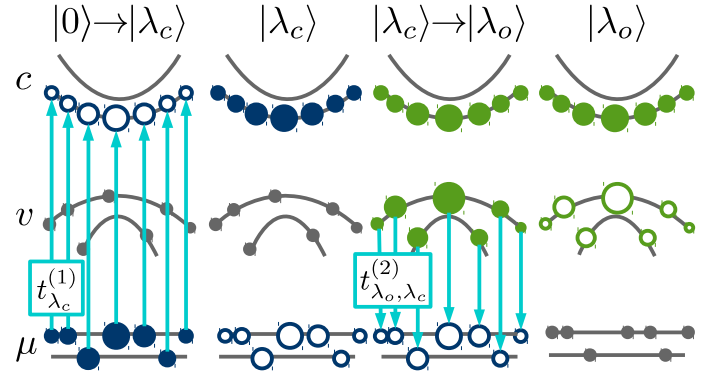


FIG. 1. Scheme of the RIXS process: A core excitation yields the intermediate many-body $|\lambda_c\rangle$, where blue circles represent the distribution of the core hole (open circles) and the excited electron (full circles). Cyan arrows indicate dipole transitions. The de-excitation from $|\lambda_c\rangle$ yields the final many-body state $|\lambda_o\rangle$. The final state is represented by green circles, where the valence hole distribution is shown in open green circles, the distribution of the excited electron in full ones.

26]. Furthermore, the process requires not only an accurate treatment of both the intermediate state, which comprises the core hole and an excited electron, as well as the final state, containing the valence hole and an excited electron, but also for the the x-ray emission that connects the two many-body states in the RIXS process.

In this Letter, we propose a novel compact analytical expression for the RIXS cross section that combines the oscillator strength of the x-ray absorption with the excitation pathways from all possible intermediate to all possible final many-body states. These pathways determine how the intermediate many-body states relax to the final one, and yield an intuitive interpretation of the RIXS process, while still including excitonic effects. To derive explicit expressions for the corresponding oscillator strength and the coherent emission pathway, we make use of the eigenstates $A_{cv,\lambda}$ of the BSE Hamiltonian, *i.e.* $H^{BSE} A_\lambda = E_\lambda A_\lambda$.

The RIXS process is described by the second-order term in a perturbative expansion of the electron-photon interaction. The *double differential cross section* (DDCS) $\frac{d^2\sigma}{d\Omega d\omega'}$ of scattering an x-ray photon with energy ω and polarization \mathbf{e}_1 , such that an x-ray photon with energy ω' and polarization \mathbf{e}_2 is emitted, is given by the Heisenberg-Kramers formula [27] as

$$\frac{d^2\sigma}{d\Omega d\omega'} \propto \sum_F \left| \sum_I \frac{\langle F | \hat{D}^\dagger(\mathbf{e}_2) | I \rangle \langle I | \hat{D}(\mathbf{e}_1) | 0 \rangle}{\omega - E_I + i\eta_I} \right|^2 \times \delta(E_F - E_0 + \omega' - \omega), \quad (1)$$

where the initial absorption leads to the excitation from the many-body groundstate $|0\rangle$ with energy E_0 to an intermediate state $|I\rangle$ with energy E_I . The emission of an x-ray photon leads to the de-excitation into the final state $|F\rangle$ with energy E_F . Here, $\hat{D}(\mathbf{e})$ describes the dipole transition operator for a given polarization \mathbf{e} .

Employing the eigenstates $A_{c\mu,\lambda_c}$ with excitation energy E^{λ_c} of the core-level BSE, we define the oscillator strength of core absorption $t_{\lambda_c}^{(1)}$ as

$$t_{\lambda_c}^{(1)} = \sum_{c\mu\mathbf{k}} [A_{c\mu\mathbf{k},\lambda_c}]^* d_{c\mu\mathbf{k}}, \quad (2)$$

where c are the conduction states of the system, μ the core states, and $d_{c\mu\mathbf{k}}(\mathbf{e}) = \mathbf{e} \cdot \langle c\mathbf{k} | \mathbf{p} | \mu\mathbf{k} \rangle$ the momentum matrix elements. With $t_{\lambda_o,\lambda_c}^{(2)}$ we define the excitation pathway from the core-level excitation λ_c to the valence excitation λ_o as

$$t_{\lambda_o,\lambda_c}^{(2)} = \sum_{c\nu\mathbf{k}} \sum_{\mu} [A_{c\nu\mathbf{k},\lambda_o}]^* d'_{\mu\nu\mathbf{k}} A_{c\mu\mathbf{k},\lambda_c}. \quad (3)$$

This definition allows us to finally write the RIXS cross section as

$$\frac{d^2\sigma}{d\Omega d\omega'} \propto \text{Im} \sum_{\lambda_o} \frac{\left| \sum_{\lambda_c} \frac{t_{\lambda_o,\lambda_c}^{(2)} t_{\lambda_c}^{(1)}}{E^{\lambda_c} - (\omega - \omega') - i\eta} \right|^2}{E^{\lambda_o} - (\omega - \omega') - i\eta} = \quad (4)$$

$$= \text{Im} \sum_{\lambda_o} \frac{|t_{\lambda_o}^{(3)}(\omega)|^2}{E^{\lambda_o} - (\omega - \omega') - i\eta}, \quad (5)$$

where we have introduced the RIXS oscillator strength $t_{\lambda_o}^{(3)}(\omega)$.

This compact expression of the DDCS has two advantages: First, it neatly separates terms that depend on either the excitation energy ω or the energy loss $\omega - \omega'$ from those that are independent of energy. This allows for an efficient numerical evaluation since the most-involved term, $t_{\lambda_o,\lambda_c}^{(2)}$, is frequency independent. More importantly, the expression yields an intuitive interpretation of the RIXS spectra in terms of *excitonic pathways* as shown in Fig. 1. In essence, the rate of the initial x-ray absorption event is given by $t_{\lambda_c}^{(1)}$, together with the energy

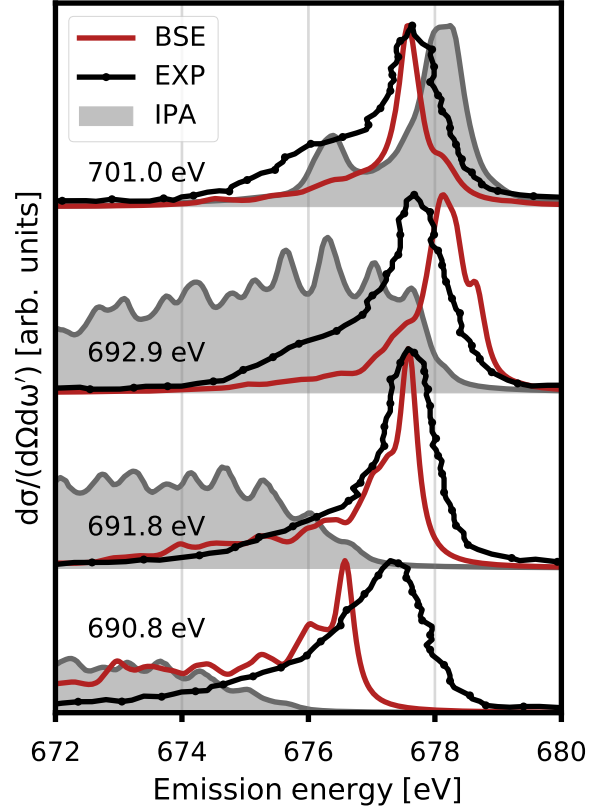


FIG. 2. Calculated (red) and experimental (black)[28] RIXS spectrum of the fluorine K edge in LiF. Both spectra are normalized for each absorption energy. A Lorentzian broadening of 0.15 eV is employed in the calculated spectra.

conservation enforced by the denominator $E^{\lambda_o} - \omega + i\eta$ in Eq. 4. The absorption leads to an intermediate state $|\lambda_c\rangle$ [31] containing a core hole, schematically shown in Fig. 1. The final RIXS spectrum is given by the rate of the first event combined with the pathway $t_{\lambda_o,\lambda_c}^{(2)}$ that connects the excited state $|\lambda_c\rangle$ with the final state $|\lambda_o\rangle$ shown in Fig. 1. The pathways $t_{\lambda_o,\lambda_c}^{(2)}$ depend strongly on the intermediate state $|\lambda_o\rangle$ due to the coherence of the absorption and emission processes, and the mixing between $t_{\lambda_c}^{(1)}$ and $t_{\lambda_o,\lambda_c}^{(2)}$ can result in destructive or constructive interference, attesting the many-body character of such processes. Another way to look at the DDCS is provided by Eq. 5 which tells that the overall RIXS signal is given by the combination of the energy loss and the oscillator strength $t_{\lambda_o}^{(3)}(\omega)$ of the whole process. The oscillator strength $t_{\lambda_o}^{(3)}(\omega)$ thus solely depends on the excitation energy, while the dependence on the energy loss is given by the denominator $E^{\lambda_o} - (\omega - \omega') + i\eta$.

Following the equations above, the determination of the RIXS DDCS requires the output of two BSE calculations: The first BSE calculation is performed to obtain the core excitations at a specific edge, which yields

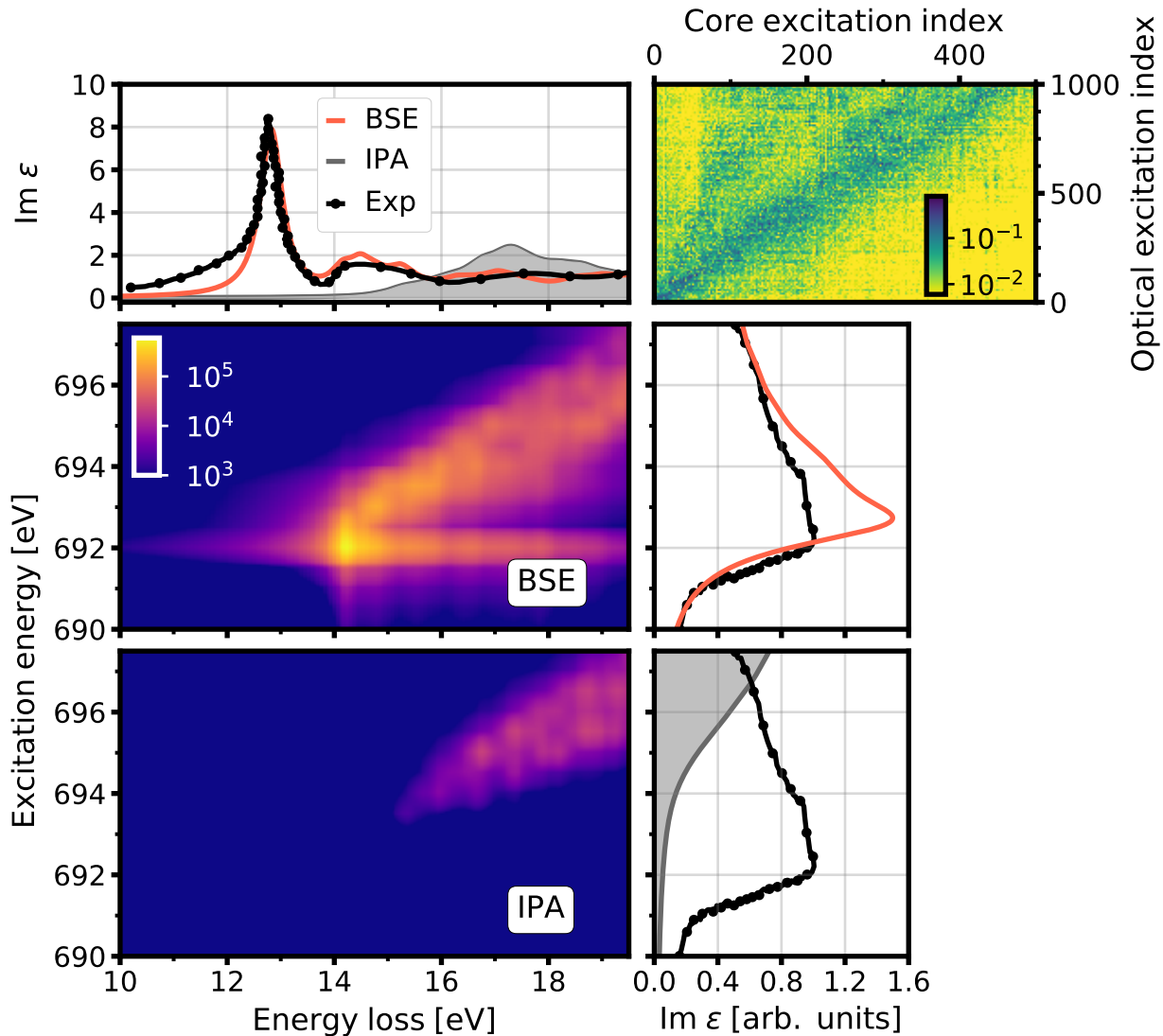


FIG. 3. F K edge RIXS cross section calculated from the BSE (center top) and within the IPA (center bottom), together with the optical (top left) and the F K edge (right) absorption spectrum. The calculated spectra (red BSE, gray IPA) are compared to experimental results (black) for the optical [29] and core [30] excitations. The excitation pathways $|t^{(2)}|^2$ between the first 500 core and 1000 optical excitations are shown on the top right.

E^{λ_c} , $A_{c\mu\mathbf{k},\lambda_c}$ as well as the momentum matrix elements $d_{c\mu\mathbf{k}}$ and $d'_{\mu\nu\mathbf{k}}$. A second BSE calculation determines the valence excitations yielding E^{λ_o} , $A_{o\nu\mathbf{k},\lambda_o}$. Subsequently, the absorption oscillator strength $t_{\lambda_c}^{(1)}$ and the pathway $t_{\lambda_o,\lambda_c}^{(2)}$ are calculated. Finally, all intermediate quantities are combined to construct the RIXS oscillator strength $t_{\lambda}^{(3)}(\omega)$ and the DDCS of Eq. 4. For a consistent treatment of the BSE eigenstates in the optical and x-ray region, we perform the calculations using the all-electron many-body implementation in the `exciting` code [32, 33]. The all-electron implementation also directly yields the momentum matrix elements $d_{c\mu\mathbf{k}}$ and $d'_{\mu\nu\mathbf{k}}$ between core states and conduction and valence

states, respectively.

To illustrate our approach, we present in the following results for the F K edge of LiF. Due to its large bandgap, strong effects of electron-hole interaction are observed, as indicated by the presence of bound excitons in both the valence and the core regimes. The calculated RIXS spectra as a function of the emission energy are shown in Fig. 2 for selected excitation energies. For an excitation energy of 690.8 eV, below the absorption onset of approximately 691.8 eV, the calculated spectrum has a peak at 676.8 eV, which slowly decays at lower emission energies, *i.e.* the maximum of the scattering occurs at a loss of 14 eV, with considerable contributions at higher energy loss. With increasing excitation energy,

the peak becomes narrower and moves to slightly higher emission energy. The broad feature at lower emission energy is strongly suppressed for excitations of approximately 691.8 eV, while a shoulder in the emission appears for even higher excitations. The calculated spectra at a given excitation energy, as well as the change as a function of the excitation energy are in good agreement with their experimental counterparts [28].

Our approach allows for a deeper analysis of the RIXS spectra, the results of which are shown in Fig. 3. For excitation energies below the absorption onset of the core edge, i.e., at approximately 691.8 eV, the cross section is small, since the F $1s$ states are not excited resonantly. This case is discussed in the Supplementary Information. When the excitation energy is in resonance with the absorption onset, the spectrum changes abruptly. The oscillator strength increases tremendously and is shifted to a distinct loss peak at 14.6 eV. For higher absorption energies, this peak shows a linear dispersion. It corresponds to the strong emission observed for absorption energies of 691.8, 692.8, and 701 eV in Fig. 2. Furthermore, this feature loses oscillator strength and widens with increasing excitation energy, thus introducing a shoulder at higher loss with increasing relative intensity.

As the shape of the RIXS spectrum is determined by the excitation pathways, we now have a closer look at the $t^{(2)}$ -matrix. The top right of Fig. 3 shows this matrix for the first 500 core and 1000 valence excitations, which determine the RIXS cross sections for excitation energies between 680.1 and 696.7 eV and energy losses between 12.8 and 18.3 eV. It shows a pronounced band-matrix form, *i.e.* the largest contributions are observed along the diagonal. From Eq. 3, two factors can be inferred that lead to large pathway matrix elements. First, the transition from the valence hole distribution of the final state to the core hole has to be dipole-allowed, and second, the distributions of the excited electron of the intermediate and final state have to be similar. For core excitations with increasing energy, the excited electron is distributed farther from the band gap, and the same holds true for optical excitations with increasing energy. This similarity leads to the band-matrix form of $t^{(2)}$. Moreover, we find that for core excitations at higher energies, pathways to more and more valence excitations are possible, and therefore the shoulder at higher loss is getting more pronounced.

Although the elements of $t^{(2)}$ yield insight into the origin of the features in the RIXS spectrum, they do not solely define it. While the pathway between the lowest excitations in the optical and core spectrum is very strong, surprisingly, the excitonic peak that dominates the optical absorption spectrum at 12.7 eV is not observed in the RIXS spectrum. This strongly bound exciton is formed by a complicate interplay of the bottom of the conduction band, dominated by the Li s states, and the top of the valence band, formed by the F p states.[34]

In the corresponding RIXS spectrum, the core excitation into the Li s states at the bottom of the conduction band is not possible, as $s \rightarrow s$ transitions are dipole-forbidden. While the $t^{(2)}$ matrix element between the dark exciton in the F K edge and the bound exciton in the optical spectrum is considerable, the $t^{(1)}$ entries are zero, as the initial excitation of the dark exciton is prohibited.

Finally, we demonstrate the importance of electron-hole interaction by comparing in Fig. 2 the RIXS spectra obtained by the BSE with those from the independent-particle approximation (IPA). For low excitation energies, a broad emission spectrum is predicted within the IPA, missing the pronounced peak found in both the experimental spectra and our BSE calculations. At an excitation energy of 701 eV, the agreement between the IPA and BSE spectra improves, because the effect of electron-hole interaction decreases with increasing excitation energy. Comparing in Fig. 3 the RIXS cross sections obtained from the two calculations, one notices that the strong peak at the excitation energy of 691.8 eV and the loss of 14.8 eV is completely missing within the IPA. This comparison demonstrates that the renormalization of the RIXS spectra at low excitation energies and low energy loss due to electron-hole interaction is considerable, which contributes the dominant feature in the RIXS cross section. We note that in the literature, this peak has been ascribed to an excitonic peak [28]. Our first-principles approach shows that RIXS spectrum at the core onset is more complex and requires in-depth analysis to be unraveled.

In conclusion, we have presented in this Letter a novel many-body expression for the RIXS cross section in condensed-matter systems. Our all-electron full-potential approach to RIXS treats the electron-hole interaction in both core and valence excitations consistently, and we show that this careful treatment of this interaction is paramount to accurately predict the RIXS cross section. Our results for the wide-gap insulator LiF are in good agreement with experiment. Importantly, our approach represents a new powerful analysis tool that allows us to track spectral features back to the coherent pathways between core and valence excitations, a crucial step to explain and interpret the richness of RIXS spectra.

This work was supported by STSM grants of the COST Action MP1306 and COST Action CA17126.

* vorwerk@physik.hu-berlin.de

- [1] A. Kotani and S. Shin, *Reviews of Modern Physics* **73**, 203 (2001).
- [2] L. J. P. Ament, M. van Veenendaal, T. P. Devereaux, J. P. Hill, and J. van den Brink, *Reviews of Modern Physics* **83**, 705 (2011).
- [3] G. Ghiringhelli et al., *Journal of Physics: Condensed*

- Matter **17**, 5397 (2005).
- [4] R.-P. Wang et al., The Journal of Physical Chemistry C **121**, 24919 (2017).
- [5] A. Cesar et al., The Journal of Chemical Physics **106**, 3439 (1997).
- [6] F. Hennies et al., Physical Review A **76**, 032505 (2007).
- [7] I. Josefsson et al., The Journal of Physical Chemistry Letters **3**, 3565 (2012).
- [8] Y. Ma et al., Phys. Rev. Lett. **69**, 2598 (1992).
- [9] Y. Ma, Phys. Rev. B **49**, 5799 (1994).
- [10] P. D. Johnson and Y. Ma, Phys. Rev. B **49**, 5024 (1994).
- [11] J. J. Jia et al., Phys. Rev. Lett. **76**, 4054 (1996).
- [12] V. N. Strocov et al., physica status solidi (b) **241**, R27 (2004).
- [13] V. N. Strocov et al., Physical Review B **72**, 085221 (2005).
- [14] M. Magnuson, M. Mattesini, C. Höglund, J. Birch, and L. Hultman, Physical Review B **81**, 085125 (2010).
- [15] E. L. Shirley, Phys. Rev. Lett. **80**, 794 (1998).
- [16] E. L. Shirley, Journal of Electron Spectroscopy and Related Phenomena **110-111**, 305 (2000).
- [17] J. Vinson, T. Jach, M. Müller, R. Unterumsberger, and B. Beckhoff, Phys. Rev. B **94**, 035163 (2016).
- [18] J. Vinson, T. Jach, M. Müller, R. Unterumsberger, and B. Beckhoff, Physical Review B **96**, 205116 (2017).
- [19] A. Geondzhian and K. Gilmore, Physical Review B **98**, 214305 (2018).
- [20] L. Hedin, Physical Review **139**, A796 (1965).
- [21] M. S. Hybertsen and S. G. Louie, Phys. Rev. Lett. **55**, 1418 (1985).
- [22] G. Strinati, Riv. Nuovo Cimento **11**, 1 (1988).
- [23] G. Onida, L. Reining, R. W. Godby, R. Del Sole, and W. Andreoni, Phys. Rev. Lett. **75**, 818 (1995).
- [24] S. Albrecht, G. Onida, and L. Reining, Phys. Rev. B **55**, 10278 (1997).
- [25] L. X. Benedict, E. L. Shirley, and R. B. Bohn, Phys. Rev. Lett. **80**, 4514 (1998).
- [26] M. Rohlfing and S. G. Louie, Phys. Rev. Lett. **81**, 2312 (1998).
- [27] H. A. Kramers and W. Heisenberg, Z. Phys. **31**, 681 (1925).
- [28] A. Kikas et al., Phys. Rev. B **70**, 085102 (2004).
- [29] K. K. Rao, T. J. Moravec, J. C. Rife, and R. N. Dexter, Phys. Rev. B **12**, 5937 (1975).
- [30] Y. Joly, C. Cavallari, S. A. Guda, and C. J. Sahle, Journal of Chemical Theory and Computation **13**, 2172 (2017).
- [31] Within the Tamm-Dancoff approximation, the excited state is given as $|\lambda\rangle = \sum_{c\mu\mathbf{k}} A_{c\mu\mathbf{k},\lambda} \hat{c}_{c\mathbf{k}}^\dagger \hat{c}_{\mu\mathbf{k}} |0\rangle$.
- [32] C. Vorwerk, B. Aurich, C. Cocchi, and C. Draxl, Electronic Structure **1**, 037001 (2019).
- [33] A. Gulans et al., J. Phys. Condens. Matter. **26**, 363202 (2014).
- [34] M. Gatti and F. Sottile, Phys. Rev. B **88**, 155113 (2013).